Complexes of HIV-1 Reverse Transcriptase with Inhibitors of the HEPT Series Reveal Conformational Changes Relevant to the Design of Potent Non-Nucleoside Inhibitors

Andrew L. Hopkins,[†] Jingshan Ren,[†] Robert M. Esnouf,[†,‡] Benjamin E. Willcox,[†] E. Yvonne Jones,[†,‡] Carl Ross,[§] Tadashi Miyasaka,[⊥] Richard T. Walker,[∥] Hiromichi Tanaka,[⊥] David K. Stammers,[§] and David I. Stuart*[,†,‡]

The Laboratory of Molecular Biophysics, Rex Richards Building, South Parks Road, Oxford, OX1 3QU, U.K., The Oxford Centre for Molecular Sciences, New Chemistry Building, South Parks Road, Oxford, OX1 3QT, U.K., Structural Biology Group, The Glaxo-Wellcome Research Laboratories, Langley Court, Beckenham, Kent, BR3 3BS, U.K., School of Pharmaceutical Sciences, Showa University, Hatanodai 1-5-8, Shinagawa-ku, Tokyo 142, Japan, and School of Chemistry, The University of Birmingham, Edgbaston, Birmingham, B15 2TT, U.K.

Received January 17, 1996[⊗]

Crystal structures of HIV-1 reverse transcriptase (RT) complexed with a range of chemically diverse non-nucleoside inhibitors (NNIs) have shown a single pocket in which the inhibitors bind and details of the inhibitor−protein interactions. To delineate the structural requirements for an effective inhibitor, we have determined the structures of three closely related NNIs which vary widely in their potencies. Crystal structures of HIV-1 RT complexed with two very potent inhibitors, MKC-442 and TNK-651, at 2.55 Å resolution complement our previous analysis of the complex with the less effective inhibitor, HEPT. These structures reveal conformational changes which correlate with changes in potency. We suggest that a major determinant of increased potency in the analogues of HEPT is an improved interaction between residue Tyr181 in the protein and the 6-benzyl ring of the inhibitors which stabilizes the structure of the complex. This arises through a conformational switching of the protein structure triggered by the steric bulk of the 5-substituent of the inhibitor pyrimidine ring.

Introduction

The virally encoded reverse transcriptase (RT) of HIV provides an important target for the development of anti-AIDS drugs. It plays a multifunctional role in the conversion of the single-stranded RNA viral genome to double-stranded DNA. Present chemotherapeutic agents against HIV-1 RT interfere with the polymerase activity of the enzyme and can be divided into two classes: nucleoside and non-nucleoside inhibitors. Nucleoside inhibitors such as AZT,[1] ddC,[2] ddI,[3] and 3TC,[4] in their metabolically activated triphosphate form compete with the nucleoside substrate and are incorporated into the primer-strand DNA causing premature chain termination.[5] Treatment of AIDS with AZT can prolong the patient's life,[6] but adverse reactions[7] and the emergence of drug-resistant viral mutants limit the effectiveness of long-term administration.[8−10] In contrast, the non-nucleoside inhibitors (NNIs) are structurally diverse aromatic compounds such as HEPT,[11] nevirapine,[12] pyridinones,[13] BHAP,[14] TIBO,[15] and thiocarboxanilides.[16] NNIs are highly specific: the absence of binding to cellular polymerases results in considerably lower toxicity than is associated with nucleoside analogues; however, this specificity also precludes the binding of most NNIs to HIV-2 RT. Kinetic[17−19] and structural[20−25] studies reveal that NNIs inhibit the enzyme noncompetitively, binding to an allosteric site some 10 Å from the polymerase catalytic site. The separate mechanisms of inhibition lead to synergism between the NNIs and the nucleoside inhibitors.[26]

With their combination of high potency, low toxicity, and exquisite selectivity, the NNIs were initially considered as candidates for AIDS monotherapy. However, their effectiveness is weakened by the very rapid development of drug-resistance mutations, *in vitro* and *in vivo*, both in monotherapy and in multidrug trials.[27−29] For many NNIs, the virus can escape drug sensitivity by a single mutation (such as Tyr181Cys, Tyr188Cys, Lys103Asn or Leu100Ile). The relatively low replication fidelity of RT[30] and the turbulent *in vivo* population dynamics of HIV[31,32] help to explain the rapid evolution of drug-resistant strains. Nevertheless, NNIs may have a role in combination therapy with nucleoside drugs since some NNI-resistance mutations (notably Tyr-181Cys) restore AZT sensitivity to a previously AZT-resistant virus.[33,34]

To improve rationally the efficacy of the non-nucleoside inhibitors, it is important to have a precise and detailed understanding of the important inhibitor−protein interactions. In an effort to dissect out these interactions, we have previously determined the crystal structures of a number of different NNIs (nevirapine, α-APA,[35] HEPT, 1051U91,[36] and 9-Cl-TIBO) in complex with HIV-1 RT.[22,25] By considering the common features observed with these chemically divergent compounds, we have attempted a definition of the functional roles of particular groups. However, the structural diversity of these NNIs, which lent generality to our conclusions, only allowed qualitative insights to be gained. To get closer to a quantitative understanding of the structural requirements for a powerful inhibitor, we have extended our studies to include a series of compounds which show widely different potencies despite their chemical similarity.

The compounds studied (Figure 1) belong to the HEPT chemical series.[11,37−40] HEPT, or 1-[(2-hydroxyethoxy)-

[†] The Laboratory of Molecular Biophysics.
[‡] The Oxford Centre for Molecular Sciences.
[§] The Glaxo-Wellcome Research Laboratories.
[⊥] Showa University.
[∥] The University of Birmingham.
[⊗] Abstract published in *Advance ACS Abstracts,* March 15, 1996.

0022-2623/96/1839-1589$12.00/0

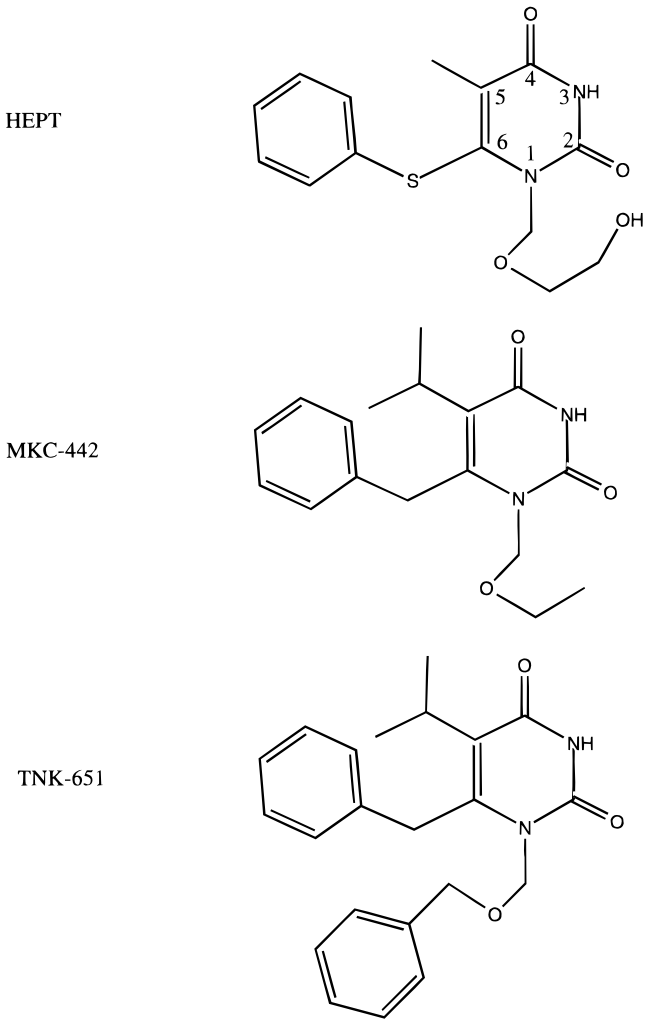

Figure 1. The chemical structures of the three RT inhibitors studied: HEPT, MKC-442, and TNK-651. The numbering of substituents is shown for HEPT. Figures 1 and 4 produced using CSC ChemDraw (Cambridge Scientific Computing Inc., Cambridge, MA).

methyl]-6-(phenylthio)thymine, was one of the earliest NNIs discovered but inhibits HIV-1 RT relatively weakly (IC_{50} = 17 μM).[11,41] MKC-442, or 6-benzyl-1-(ethoxymethyl)-5-isopropyluracil (I-EBU), is a very potent inhibitor of HIV-1 RT (the IC_{50} being 2000-fold lower at 8 nM),[26,42] although only three relatively minor alterations have been made to the HEPT structure. The different spectrum of drug-resistance mutations between HEPT and MKC-442 parallels the variation in potency. A single mutation (Tyr188His) renders the virus effectively resistant to HEPT.[43] To become similarly resistant to MKC-442, however, the virus requires two mutations (Tyr181Cys with either Lys103Arg or Val108Ile), thus slowing the development of a resistant viral population.[44] The third compound, TNK-651, or 6-benzyl-1-[(benzyloxy)methyl]-5-isopropyluracil, achieves a marginal increase in potency over MKC-442 (IC_{50} = 6 nM (Baba, personal communication)) by the addition of a bulky (benzyloxy)methyl group. No resistance data for this compound are available.

We have previously described the RT−HEPT complex structure (refined against data to a resolution limit of 3 Å),[22] and have now determined crystal structures of HIV-1 RT complexed with MKC-442 and TNK-651 using data to a high-resolution limit of 2.55 Å in each case. These structural analyses explain why some small changes (*e.g.* at the 5-position of the pyrimidine ring) lead to a significant increase in potency, whereas other, larger, changes have little effect. Such effects could not have been understood from analysis of one complex structure alone, since major differences in affinity result from conformational switching of protein residues within the NNI-binding pocket. In addition, we find that neither these compounds nor the others we have studied[22,25] fully exploit the potential protein interactions available, suggesting scope for the design of improved inhibitors.

Overall Structure of the RT Complexes

The structure determination for the RT−HEPT complex has been reported.[22] X-ray diffraction data for the MKC-442 and TNK-651 complexes were collected from flash-cooled crystals using synchrotron radiation, and the structures were solved using the molecular replacement method. Electron density maps for both the MKC-442 and TNK-651 complexes show that the structures are mostly well-defined, but in each case short stretches of the polypeptide chains had to be omitted due to the absence of interpretable electron density. The current model for RT−MKC-442 complex (including 412 water molecules) has an *R* factor of 0.197 for all data in the range of 25−2.55 Å with good stereochemistry (typified by root-mean-square (rms) deviations from canonical bond lengths and angles of 0.010 Å and 1.6°, respectively). The current model for RT−TNK-651 (containing 138 water molecules) has an *R* factor of 0.207 for all data in the resolution range 20−2.55 Å with rms deviations of 0.010 Å and 1.6° for bond lengths and angles, respectively. Details of the data and models are given in Table 1. The structure determination is described in the Experimental Section.

In each case the overall structure of the RT (p66/p51) heterodimer is as reported previously for other RT−NNI complexes.[20−25] The non-nucleoside binding site is located in a pocket between the β-sheet comprising β4, β7, and β8 and the sheet comprising β9, β10, and β11 in the p66 palm domain (secondary structural elements are defined in Ren *et al.*[22]). This site is some 10 Å from the polymerase catalytic residues Asp110, Asp185, and Asp186. The internal surface of the pocket is composed mainly of hydrophobic residues with few hydrophilic residues in the vicinity of the drug. Our data show unambiguously the positions, orientations, and conformations of HEPT,[22] MKC-442 (Figure 2a), and TNK-651 (Figure 2b) within this pocket. The volumes of the NNI-binding pockets in the HEPT, MKC-442, and TNK-651 complexes are 700, 640, and 660 Å^3, respectively, of which the inhibitors occupy 260, 270, and 320 Å^3, respectively (calculations performed by the program VOLUMES, RE, unpublished, based on all atoms including hydrogen atoms and using atomic radii defined in GRASP[45]). The HEPT analogues are bound in very similar orientations with the pyrimidine and 6-benzyl rings (or 6-phenylthio ring, in the case of HEPT) occupying equivalent positions (Figure 3). Over 70% of the volume occupied by the HEPT molecule in its RT complex is also occupied by the two larger analogues in theirs.

Comparison of the RT−HEPT analogue complexes shows no significant global rearrangement, but there are important changes in the conformations of residues lining the NNI-binding pocket. Despite the variation

Table 1. Crystallographic Structure Determination Statistics

complex	RT−MKC-442	RT−TNK-651
data collection details		
data collection site	7.2, SRS, 1994	BL19, ESRF, 1995
temperature (K)	100	100
wavelength (Å)	1.488	0.930
collimation (mm)	0.20	0.21 × 0.22
number of crystals	1	1
unit cell (Å)	136.8, 109.8, 72.4	137.3, 110.2, 72.1
crystal form	E	E
data processing details		
resolution range (Å)	30.0−2.55	20.0−2.55
observations	336340	233000
unique reflections	34717	30972
completeness (%)	95.6	85.3
reflections with $F/\sigma(F) > 3$	32128	28479
R_{merge} (%)[a]	7.5	6.7
outer resolution shell		
resolution range (Å)	2.64−2.55	2.64−2.55
unique reflections	3160	2508
completeness (%)	89.5	70.6
reflections with $F/\sigma(F) > 3$	2439	1737
refinement statistics		
resolution range (Å)	25−2.55	20−2.55
unique reflections	34612	30972
R factor[b]	0.197	0.207
protein atoms	7842	7773
inhibitor atoms	22	27
water molecules	412	138
rms bond length deviation (Å)	0.010	0.010
rms bond angle deviation (deg)	1.6	1.6
mean *B* factor (Å^2)[c]	33/37/35/17	54/59/44/31
rms backbone *B* factor deviation (Å^2)[d]	3.4	5.3
residues with "most favored" (ϕ, ψ) angles (%)[e]	87.3	83.8

[a] $R_{merge} = \sum|I - \langle I\rangle|/\sum\langle I\rangle$. [b] *R* factor $= \sum|F_{obs} - F_{calc}|/\sum F_{obs}$. [c] Mean *B* factor for main chain, side chain, water, and inhibitor atoms, respectively. [d] rms deviation between *B* factors for bonded main chain atoms. [e] As defined by the program PROCHECK.[62]

in crystal unit cell dimensions for the three complexes, the domain arrangements are very similar, and we are confident that the changes observed in the NNI-binding pocket are due to the differences between inhibitors. Thus, we can relate the observed IC_{50} values to subtle differences in the inhibitor−protein interactions (Figure 4). The two key features are the discrete conformational switch of Tyr181 and the more continuous variation in the position of the "Pro236 hairpin", which comprises β9 and β10 and the turn joining them, centered on residue Pro236.

Conformational Switching at Tyr181

The most noticeable conformational disparity between the complex with HEPT and those with its two more potent analogues is the conformation of the side chain of Tyr181, which has swung around with a mean change in χ_1 of 110° (Figure 5). The side chain orientation seen in the MKC-442 complex allows improved interactions with the 6-benzyl ring of the inhibitor and other nearby aromatic residues (Figure 6). Essentially the same conformations are observed for the TNK-651 complex and for our other analyses of complexes with potent inhibitors.[22,25] We have noted that the binding of potent NNIs alters the conformations of residues Tyr181, Tyr183, and Tyr188 from those observed in the unliganded RT structure[46,47] to conformations virtually indistinguishable from those in the inactive p51 subunit of the enzyme.[47] The binding of HEPT only switches residues Tyr183 and Tyr188, leaving Tyr181 in a similar conformation to that seen in the absence of inhibitor (Figure 5). We believe that this explains the considerable increase in the binding affinities for MKC-442 and TNK-651.

The 6-benzyl/6-phenylthio rings of the HEPT series of NNIs are central to the aromatic ring interactions. The loss of interaction with Tyr181 is reflected in a 20−25° rotation between HEPT and its analogues. In this respect HEPT is also an outlier in comparison to the RT complexes with other strong inhibitors (*e.g.* nevirapine and α-APA[22]). However, the 6-phenylthio ring of HEPT could, in principle, reposition to form favorable interactions with the side chain of Tyr181 if this residue was reorientated into the p51-like conformation. The thio (rather than methylene) linkage between the two rings of HEPT does not prohibit this, since substituting different linking groups in HEPT analogues which are otherwise identical results in almost indistinguishable inhibitory effects (HT, unpublished results). Therefore, the question is why do the more effective analogues, but not HEPT itself, switch the orientation of the Tyr181 side chain?

The 5-Position Trigger

Structure−activity relationship (SAR) studies show that a 5-position substituent on the pyrimidine ring is essential for HEPT analogues to bind to RT. Replacement of the 5-methyl group of HEPT with a hydrogen atom leads to a complete loss of inhibitory properties,[41,48] while its replacement by a larger moiety, such as an ethyl or an isopropyl group (*e.g.* in MKC-442 and TNK-651), produces much more potent inhibitors.[49−51] Comparison of the HEPT analogue complexes with the structure of the drug-free RT[47] shows that it is the 5-group that perturbs the conformation of Tyr181. The 5-methyl group of HEPT produces only a slight perturbation, whereas the larger substituents of MKC-442 and TNK-651 would clash severely with Tyr181 in either the unliganded RT or RT−HEPT conformations. Thus, the 5-isopropyl group appears to force Tyr181 into the p51-like conformation, where it is then able to form strong interactions with the 6-phenyl ring of the inhibitor and

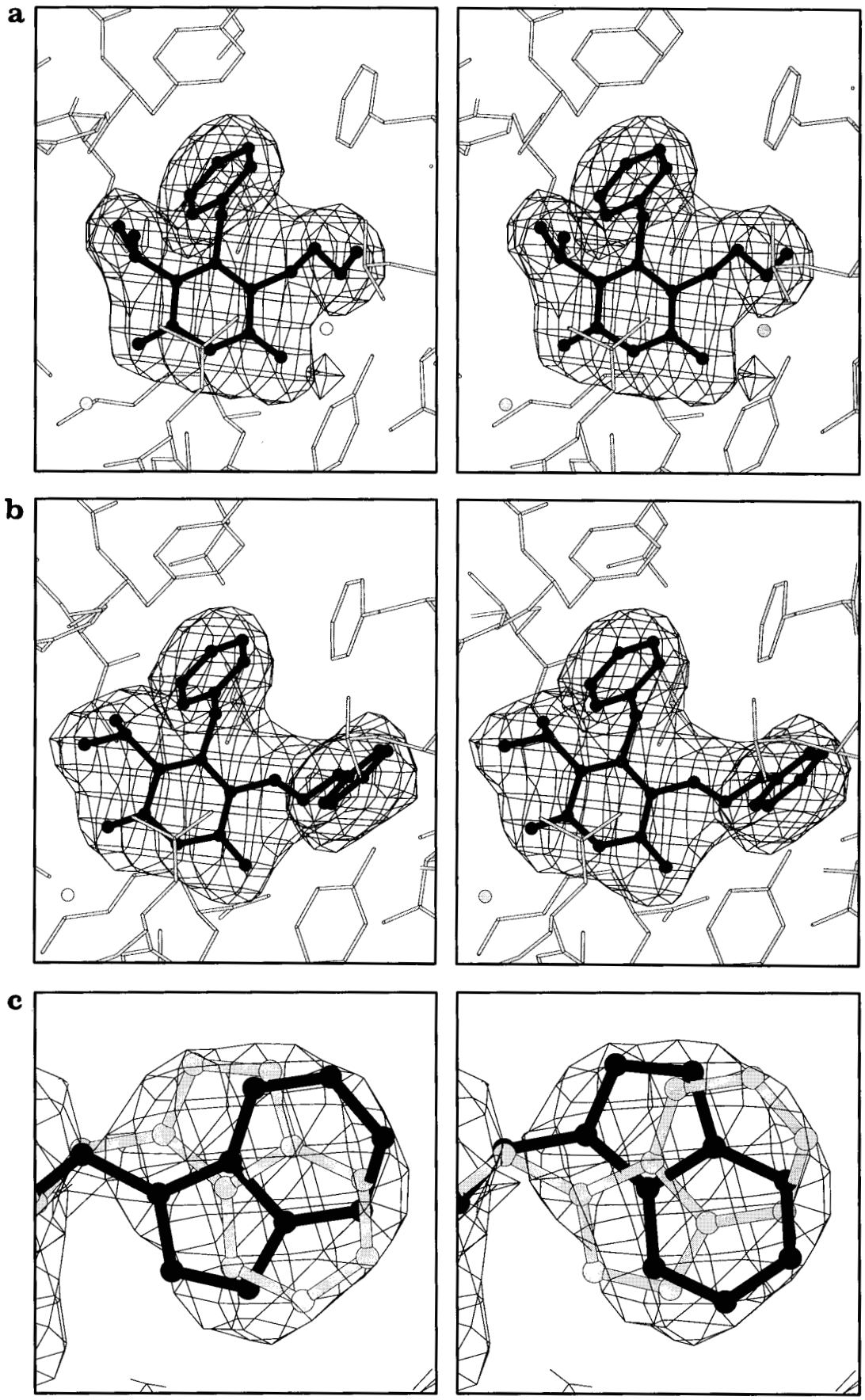

Figure 2. Electron density for the RT complexes. Parts (a) and (b) show stereodiagrams of omit $|F_{obs}| - |F_{calc}|$ electron density contoured at 3σ for MKC-442 and TNK-651, respectively. The inhibitors are shown in black and the surrounding protein structure in gray. Spheres show the position of electron density attributed to bound water molecules. Maps were phased using models from which the inhibitor had been excluded followed by further refinement. (c) $2|F_{obs}| - |F_{calc}|$ electron density contoured at 1σ for the side chain of Trp229 in the RT−MKC-442 complex. The maps were phased using the conformation in black in each case and show clear evidence for the presence of both conformers in the crystal. Figures 2, 3, and 5−8 produced using BobScript (RE (unpublished) modified from MolScript[63]). Color figures rendered with Raster3D.[64]

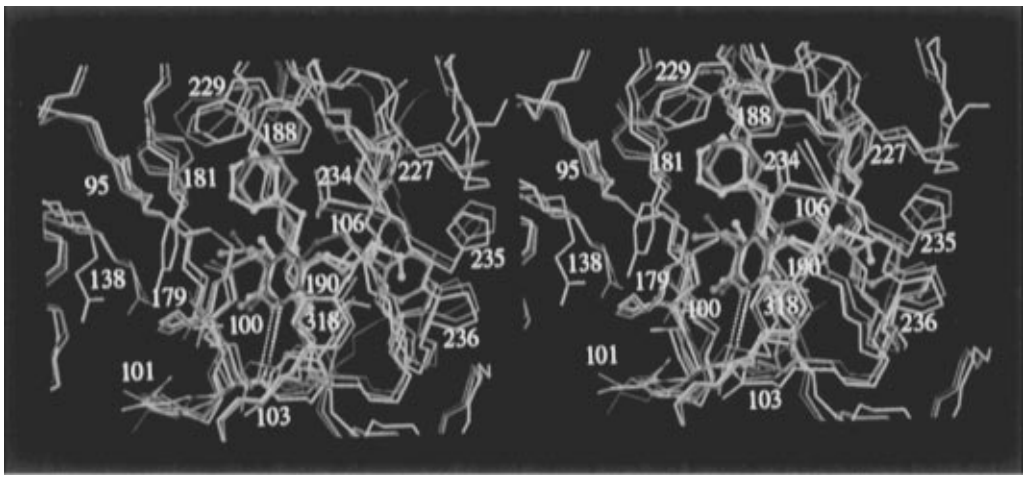

Figure 3. Stereodiagram of the superposed NNI-binding sites for the RT complexes with HEPT (blue), MKC-442 (maroon), and TNK-651 (green). The NNIs are shown as ball-and-stick representations and the surrounding protein atoms as thin lines of the same color. Side chain atoms are shown for the NNI-contact residues defined in Figure 4. Most differences in the surrounding protein structure are small, except for the change in conformation of Tyr181 in the RT−HEPT complex and the associated movement of the side chain of Glu138 from the p51 fingers domain. The conserved hydrogen bond between 3-NH of all the HEPT series inhibitors and the carbonyl oxygen of Lys101 is shown as a yellow dashed bond in each case. The relative conformations of the two rings common to all three inhibitors are defined by the dihedral angles N1−C6−*X*−C1′ (ω_1) and C6−*X*−C1′−C2′ (ω_2). For HEPT X = S, $\omega_1 = -105°$, and $\omega_2 = 185°$. For MKC-442 X = CH_2, $\omega_1 = -80°$ and $\omega_2 = 140°$. For TNK-651 X = CH_2, $\omega_1 = -95°$ and $\omega_2 = 150°$. The binding sites were separately superposed onto the structure of the RT−nevirapine complex (our highest resolution structure) to compensate for differences in crystal form and domain orientations based on the "core" of the p66 palm domain (residues 94−118, 156−215, and 225−243), residues 317−319 from the p66 connection domain, and residues 137−139 from the p51 fingers domain using the program SHP.[65]

other aromatic residues. Further evidence for a "trigger" role for these groups comes from the observation that in MKC-442 and TNK-651 the isopropyl groups adopt rotamers differing by 180°. Combined with a slight alteration in the orientation of the pyrimidine ring, the net effect is to place the isopropyl groups in exactly equivalent places in the binding pocket, in each case preserving the trigger action.

We have previously noted that all potent NNIs we have studied possess groups which occupy the same volume of space as the 5-substituent:[25] the cyclopropyl group of nevirapine, the ethyl group of 1051U91, the 5(*S*)−methyl group of 9-Cl-TIBO, and the amide group of α-APA all perform the same steric role as the 5-isopropyl groups of MKC-442 and TNK-651.

Protein Flexibility Accommodates 1-Substituent Diversity

The greatest chemical differences between the three HEPT analogues are the 1-substituents on the pyrimidine rings: in HEPT this is a (2-hydroxyethoxy)methyl group, MKC-442 possesses an ethoxymethyl group, and TNK-651 has a large (benzyloxy)methyl tail (Figure 1). This substituent is, in fact, the only difference between MKC-442 and TNK-651. The similarity in effectiveness of these two inhibitors demonstrates that the movement of the protein structure necessary to accommodate such a change can be achieved at little energetic expense. SAR studies of HEPT analogues indicate that there is a small increase in the IC_{50} if the hydrophilic hydroxyl group from the ethoxymethyl tail is replaced by a hydrophobic group,[51] as one might predict from the hydrophobic nature of this portion of the binding pocket.

In all the RT−HEPT analogue crystal structures discussed here, the substituent on N1 contacts three segments of the polypeptide chain: strand β4, the loop prior to strand β9 (residue Pro225), and the Pro236 hairpin. Strand β4 is structurally invariant in these complexes whereas the Pro225 and Pro236 loops flex to optimize contacts with the different substrates (Figure 7). With HEPT and TNK-651 the loops occupy positions similar to those observed in the structure of the unliganded enzyme.[47] In the presence of MKC-442, the loops move, contracting the binding pocket and tracking the shorter ethoxymethyl tail. The loops move partly as rigid bodies leaving a residual pocket is partially occupied by an electron-dense group which appears to form a hydrogen bond with the carbonyl oxygen of residue Lys103. We cannot be certain of the chemical identity of this group, but it may simply be a particularly well-ordered water molecule. With the other NNIs we have studied more substantial contractions around the inhibitors occur (Figure 7), in the case of these more compact inhibitors the conformation is stabilized by a hydrogen bond from the carbonyl oxygen of residue 236 to the main chain amide NH of residue Lys103. We do not know the limits of the flexibility for the Pro236 hairpin, but comparison of our RT structures shows that a shift of over 5 Å is possible for the Cγ atom of Pro236. The conformational changes appear to have two principal components. First there is a switching of the backbone torsion angles in the region of residue 233 which appears to position the remainder of the β10 strand, the loop, and much of β11 in one of two possible orientations. The second component is flexibility centered on Pro236. The net result is to allow Pro236 to select from a broad fan of positions the one that best fits the inhibitor. This shift accounts for most of the difference in volume of the NNI pockets between the various structures, with inhibitors of various sizes fitting relatively snugly.

A further difference in this region of the pocket is seen at residue Trp229; in the MKC-442 complex the electron density map clearly shows two conformations for the side chain, one similar to that in other NNI complexes (including RT−TNK-651), and the other, rotated by 180° about χ_2, similar to the conformation observed in the unliganded RT[47] (Figure 2c). This disorder appears to

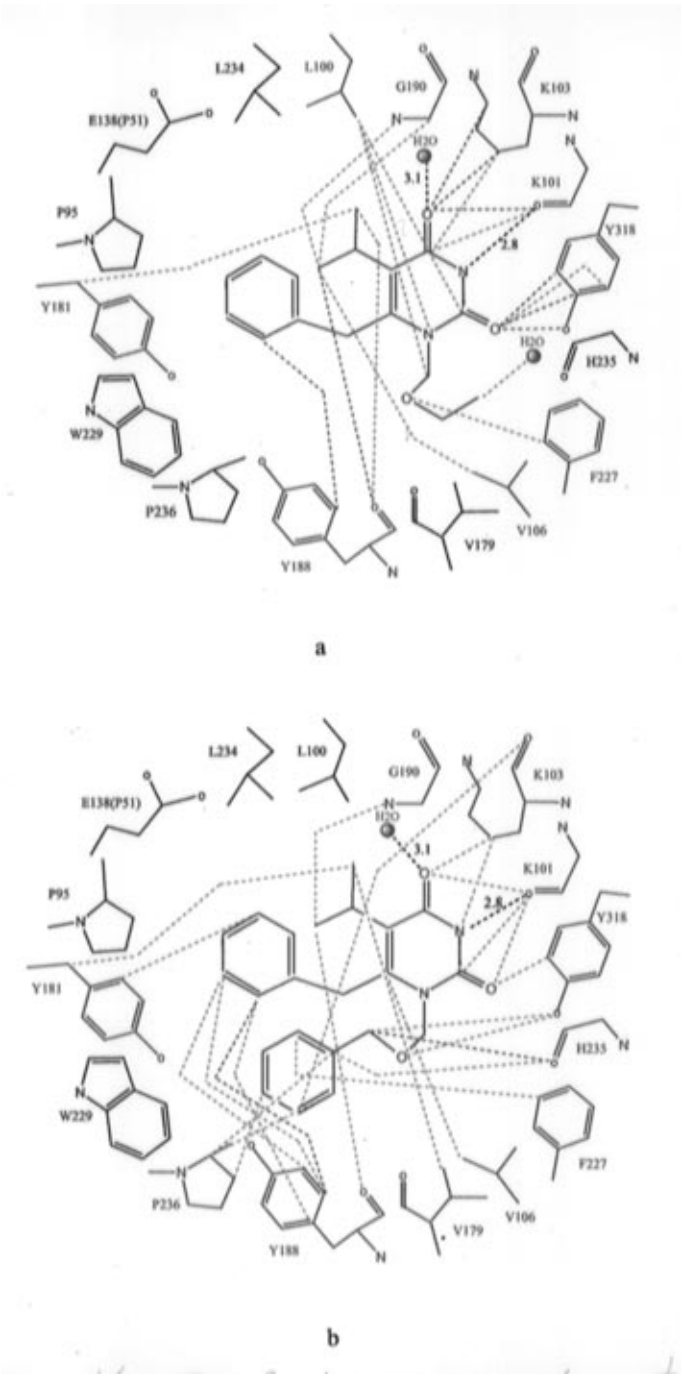

Figure 4. Schematic diagrams showing the NNIs (in red) and their interactions with the RT molecule for (a) MKC-442 and (b) TNK-651. Residues shown are those which have at least one contact (within 3.6 Å) with any of the (seven) RT NNIs we have studied. Residues contacting each NNI are shown in green, others in blue. Pink spheres represent water molecules. Individual distances between NNI and protein atoms are shown by dashed lines ($d \leq 3.3$ Å in pink; $3.3 < d \leq 3.6$ Å in light blue; potential hydrogen bonds with distances in black).

be allowed due to movement of residues 230 and 231 in the MKC-442 complex relative to the other complexes. We can offer no explanation for this movement, which increases the conformational freedom of Trp229.

Since the variation in the 1-substituent of the pyrimidine ring is the only difference between MKC-442 and TNK-651, we assume that this is the cause of the variation in the orientation of the pyrimidine ring between the two complexes (we have noted the effect of this on the orientation of the 5-substituent above; Figure 3 shows the effect). Since we can see no reason why

Figure 5. A comparison of the conformations adopted by residue Tyr181 in the superposed p66 (left) and p51 (right) palm domains in the unliganded RT molecule (yellow) and in all the RT−NNI complexes we have studied (blue, HEPT; maroon, MKC-442; green, TNK-651; gray, nevirapine, 1051U91, α-APA, and 9-Cl-TIBO). The p66 chains were superposed in the manner described in the legend to Figure 3. The p51 chains were superposed on the RT−nevirapine structure based on the whole p51 palm domain except for the terminal residues of each chain and a short region containing a disordered loop (residues 97−118, 149−209, and 234−240). In all the RT−inhibitor complexes, except with HEPT, the conformation of Tyr181 in the p66 chain is very similar to that observed in the p51. For the RT−HEPT complex the conformation is more akin to that of the unliganded RT.

the shorter 1-position tail on MKC-442 should drag the ring toward it we assume that the bulky substituent of TNK-651 pushes the ring away a little. This does not disrupt the H-bond between the pyrimidine ring of the inhibitor and the main chain carbonyl oxygen of residue Lys101. Subtle rearrangements of the torsion angles defining the relationships between the two principal rings maintain the position in space of the 6-benzyl ring very precisely. The benzyl moiety of the 1-substituent of the TNK-651 may exert some force on the position of the pyrimidine ring because of strong stacking interactions between the 1-position benzyl group and Pro236.

Polar Interactions and Hydrogen Bonds

The hydrophobic nature of the NNI pocket provides relatively few possibilities for polar interactions and hydrogen bonding between the NNIs and the protein. However, the geometry of interaction for HEPT analogues appears to be constrained by a strong hydrogen bond from the 3-NH of the pyrimidine ring to the carbonyl oxygen of Lys101 (3.1 Å for HEPT and 2.8 Å for the tight binders MKC-442 and TNK-651, Figure 3). Since there is a slight difference in the orientation of the pyrimidine ring between MKC-442 and TNK-651, maintenance of this H-bond necessitates a small movement of the polypeptide chain in the vicinity of residue Lys101. In addition, for the MKC-442 and TNK-651 complexes (where there are sufficient data to permit location of water molecules), there is a water molecule in the NNI-binding pocket situated near a channel to

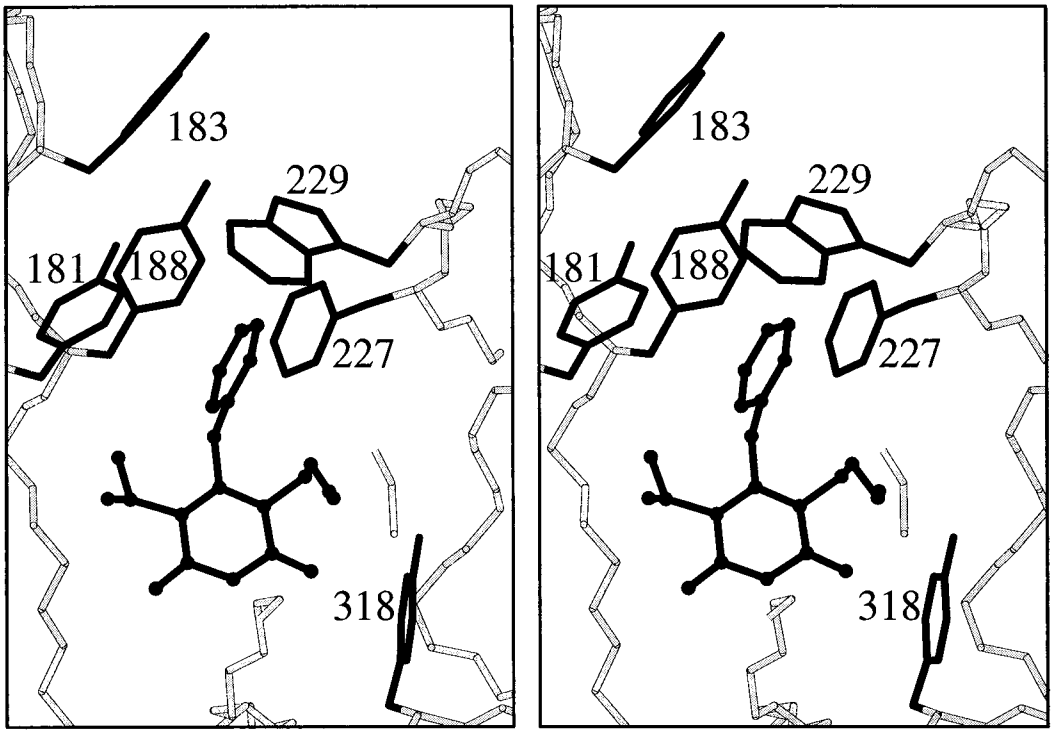

Figure 6. Stereodiagram of the aromatic residues (Phe, Trp, and Tyr) around the NNI-binding site for the RT−MKC-442 complex. MKC-442 is shown as a black ball-and-stick model and the aromatic residues as black sticks. The nearby protein main chain is shown in gray. These ring interactions are conserved for all RT−NNI complexes we have studied with the exception of Tyr181 in the RT−HEPT complex.

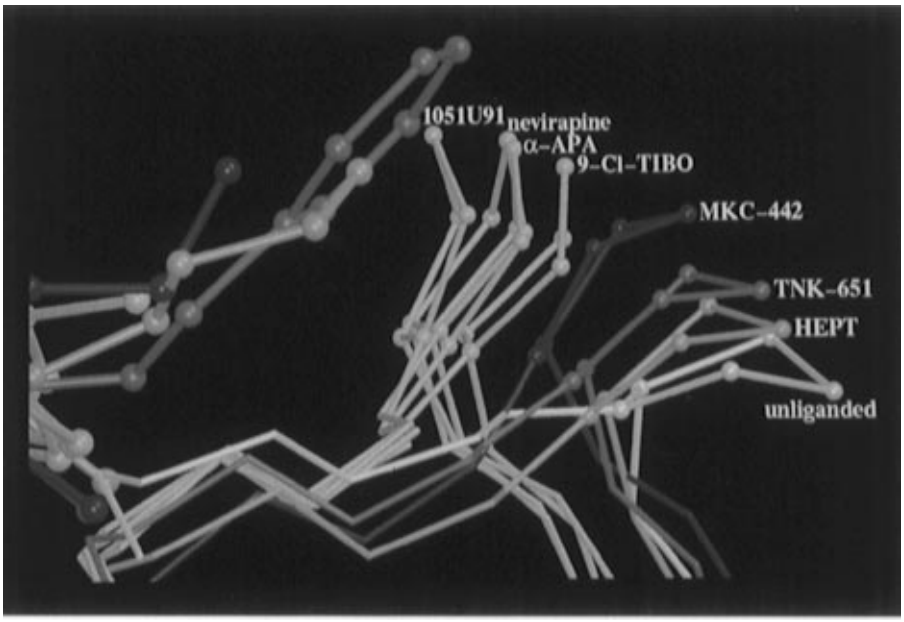

Figure 7. A comparison of the position and conformation of residue Pro236 in the superposed p66 palm domains of the unliganded and NNI-bound RT structures we have studied. The NNIs themselves are shown as ball-and-stick models with large atom spheres, the atoms comprising Pro236 are shown with small atom spheres and the main chain from residues 233−238 is shown by sticks. The color scheme is that of Figure 5, and the superposition method is described in the legend to Figure 3. The different positions of Pro236 are labeled with the name of the NNI present in the complex. For the HEPT series of inhibitors the "tail" of the inhibitor causes the Pro236 loop to retain a conformation similar to that observed in the unliganded RT structure. The extreme change in atom position (between C_γ atoms in the unliganded RT and the RT−1051U91 complex) is 5.3 Å.

the bulk solvent, which forms a triad of hydrogen bonds between the 4-carbonyl oxygen of the inhibitor, the main chain nitrogen of Lys101, and a carboxyl oxygen of Glu138 in the p51 chain. In the RT−HEPT complex, Tyr181 and Glu138 (in the p51 chain) are in conformations which could still allow a water molecule to bind in this space although in this case hydrogen bonds would be formed with the hydroxyl oxygen of Tyr181 and the side chain of Glu138 (Figure 3). We note that analogous polar interactions are seen not only in complexes with other compounds such as 9-Cl-TIBO[25] but also in the unliganded RT apo-enzyme where the hydroxyl group of Tyr188 approaches sufficiently close to the carbonyl oxygen of residue 101 to form a weak hydrogen bond, suggesting that these interactions are of considerable importance. These hydrogen bonds are particularly significant since they involve protein main chain atoms.

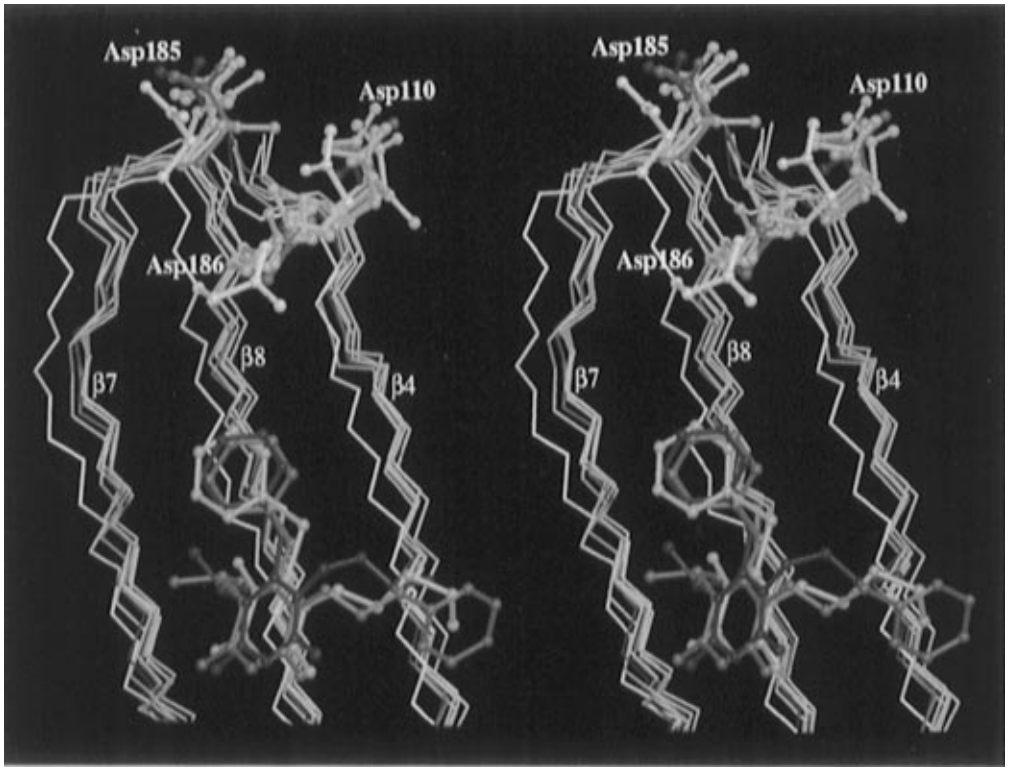

Figure 8. Stereodiagram showing how the binding of NNIs inhibits the polymerase activity of RT by repositioning the key catalytic residues Asp110, Asp185 and Asp186. Ball-and-stick models show the positions of the bound HEPT-series inhibitors and the side chain atoms of the catalytic residues in all the superposed NNI-binding sites; lines show the position of the main chain in the strands β4, β7, and β8. The color scheme is that of Figure 5, and the superposition is described in the legend to Figure 3. The movement of the catalytic aspartate residues in the RT−HEPT complex (blue) compared to the unliganded RT (yellow) is as great as with the other complexes, suggesting that the lower inhibitory action of HEPT is due to a lower binding affinity rather than a less-inhibited bound conformation.

Is Potency Due to Binding Affinity or Mechanism?

Analysis of our RT−NNI complex structures reveals that the primary structural difference in the binding site between potent and weak inhibitors is the conformation of Tyr181. Implicit in our discussion has been the assumption that the increased potency reflects tighter binding of those compounds which cause switching of the Tyr181 conformation. However, an alternative explanation is that the binding of weak inhibitors (such as HEPT) is still tight, but failure to switch Tyr181 to the p51-like conformation results in only partial inhibition. We feel that this is unlikely for the reasons outlined below.

We have previously reported that, in the crystal, the off-rate for HEPT is greater than for more effective inhibitors.[22] Indeed this formed the basis for our determination of the unliganded enzyme structure,[47] since HEPT diffuses out of crystals of the RT−HEPT complex during the crystal shrinkage procedure, whereas with other complexes the NNIs remain tightly bound. Furthermore, we know that this behavior is not due to partial steric blocking of the pocket allowing only HEPT to pass, since we have been able to diffuse a variety of inhibitors back into RT crystals (*e.g.* HEPT,[22] 9-Cl-TIBO,[25] TNK-651, and other unpublished results). This suggests that the greater off-rate for HEPT reflects much weaker binding.

It is thought that there is a common mechanism of inhibition for all NNIs: the displacement of the catalytic aspartic acid residues 110, 185, and 186 on NNI binding.[47] In the HEPT complex, this displacement is essentially the same as with other RT−NNI complexes (Figure 8). Thus, the structural evidence is that the RT−HEPT complex is no less inhibited than other RT−NNI structures. This is supported by biochemical data which show a dose−response curve for HEPT which tends toward full inhibition.[52] We conclude that the perturbation of Tyr181 affects the binding affinity of the inhibitor rather than the mechanism of inhibition.

Interpretation of Structure−Activity Relationship Data

Comparisons between the RT−NNI structures we have elucidated enables us to determine which features of the binding pocket are flexible and which are rigid when accommodating a diverse range of NNIs: Tyr181 and the Pro236 loop show the greatest flexibility, whereas most residues in strands β4, β7, and β8 and residue Tyr318 are virtually static. Such information can be used to explain SAR data for other members of the HEPT series[49−51] and to focus attention on parts of HEPT molecule which appear to be favorable targets for optimization.

In general, tight binding inhibitors make relatively nonspecific interactions with the Pro236 loop. However, it seems possible to exploit the plasticity of this part of the pocket to gain specific protein−inhibitor interactions or, alternatively, to accommodate substantial modifications of the inhibitor molecule which improve its pharmacokinetic properties without a significant loss of binding affinity. Large substituents may, however, render binding sensitive to mutations in this region of the pocket (sensitivity to a Pro236Leu mutation has been reported for BHAP[53]).

Two further modifications to the basic HEPT molecule have been found which are generally favorable: replacement of the 2-carbonyl group by a thiocarbonyl group[48,54] and addition of *m*-dimethyl groups to the 6-benzyl ring.[38,50] In our structures, the 2-carbonyl oxygen points toward the face of Tyr318, and replacement of this oxygen by a more polarizable sulfur atom would be expected to create a more favorable dispersion interaction. Furthermore, the energy required to desolvate a carbonyl group will be greater than for a thiocarbonyl group which cannot form such strong interactions with water. The *m*-dimethyl substituents on the 6-benzyl ring are in a position to make favorable van der Waals contacts with Trp229 at the "roof" of the binding pocket. We note that, thus far, this residue has remained conserved despite presumed selection pressure from NNIs. The roof of the pocket has a particularly hydrophobic surface (comprising residues Tyr181, Tyr188, Phe227, and Trp229), and we observe that significant nearby volume remains unexploited. Although the presence of *m*-dimethyl substituents is metabolically unfavorable, being open to electrophilic attack, this ring is an attractive target for further optimization. It may even be possible to accommodate a 6-naphthalylmethyl group as a replacement for the 6-benzyl group.

Conclusions

Many NNIs have been synthesized in the quest for new anti-AIDS therapies. These appear to work by a common inhibitory mechanism.[47] The pocket in which all NNIs bind is created, presumably on NNI entry, by a conformational switch of key residues to mimic the inactive polymerase site in the p51 chain.[47] With HEPT this conversion is only partial, the position of Tyr181 only being slightly perturbed. We suggest that this weakens the binding of HEPT rather than making the drug-bound enzyme conformation less inhibited. With the HEPT series of NNIs the trigger for the conformational switch of Tyr181 is the bulk of the 5-substituent: a methyl group is not large enough to force Tyr181 to move.

While the Tyr181 switch appears to be the major determinant of NNI activity, there is another part of the protein structure which changes depending on the NNI: the Pro236 loop. This flexible loop forms few contacts with the rest of the protein, but in the presence of an NNI it is drawn toward the inhibitor, apparently due to the hydrophobic nature of the residues in the loop. Although the position of the loop varies substantially between different NNIs, this seems to involve little energetic cost, and only marginal changes in NNI activity can be related to the Pro236 conformation.

The emergence of NNI-resistant viral populations is rapid: days or weeks at best. Since the NNI pocket is not associated with the enzymatic function of RT, many changes to the residues lining it still result in viable enzyme. However, the virus does not have *carte blanche*: mutations resulting in more bulky side chains (such as Gly190Glu which renders the enzyme significantly less active[55]) could distort the polymerase catalytic site in an analogous way to the NNIs. Thus, typical mutations contract the side chains away from NNIs leading to a loss of binding energy rather than excluding the NNI from the pocket. With the weaker inhibitors (such as HEPT) a single lost interaction is enough to confer effective resistance, whereas more powerful inhibitors may require two changes.

Many attempts to understand NNI function have been made, but unless such studies can take protein flexibility into account, they are doomed. Structure determination provides the only way of probing this flexibility. The major changes which create the NNI pocket are the same with all inhibitors, and we have observed that some NNIs mold themselves to fit the pocket.[25] However, unexpected variation in protein structure can occur, such as the conformational switching of Tyr181, and by elucidating a spectrum of RT−NNI complex structures, we believe we are beginning to achieve an understanding of the processes involved. The next task is to apply this understanding to the design of inhibitors which can withstand at least the more facile resistance strategies of HIV.

Experimental Section

Synthesis of Compounds. The syntheses of HEPT and MKC-442 were performed according to the published procedures.[39,56] TNK-651 was prepared from MKC-442 by the following series of reactions: N3-phenacylation, hydrolysis of the N1-ethoxymethyl group, N1-(benzyloxy)methylation, and removal of the N3-phenacyl group.[56]

Physical data of TNK-651 are as follows: mp 112−113 °C (ether); ^{1}H NMR ($CDCl_3$) δ 1.27 (6H, d, J = 7.0 Hz, CHMe_2), 2.85 (1H, m, CHMe$_2$), 4.17 (2H, s, 6-CH_2Ph), 4.66 (2H, s, OCH_2-Ph), 5.21 (2H, br, NCH_2O), 7.06 (2H, d, J = 7.3 Hz, Ph), 7.24−7.36 (8H, m, Ph), 8.52 (1H, br, NH); FAB-MS m/z 365 (M^+ + H). Anal. Calcd for $C_{22}H_{24}N_2O_3$: C, 72.51; H, 6.64; N, 7.69. Found: C, 72.46; H, 6.65; N, 7.60.

Preparation of Crystals. Orthorhombic crystals (space group $P2_12_12_1$) of the RT−MKC-442 and RT−TNK-651 complexes were grown (using our previously reported cocrystallization protocol[57]) at 4 °C by equilibration against reservoirs of 6% polyethylene glycol (PEG) 3400 with a standard McIlvane pH 5.0 citrate−phosphate buffer (24.25 mM citric acid, 51.5 mM Na_2HPO_4) using the sitting drop method. The crystals were partially dehydrated by equilibration against 46% PEG 3400 over a period of 3 days and then stored in the dehydrating solution until use. This procedure increased the order in the crystals, allowing measurement of higher resolution data, and provided a cryoprotectant for flash cooling.

X-ray Data Collection and Processing. Diffraction data for the RT−MKC-442 complex were collected in November 1994 on Station 7.2 at the SRS, Daresbury Laboratory, U.K., using the oscillation method. Data frames of 1.5° oscillations were recorded using an 18 cm MAR Research imaging plate placed 130 mm from the crystal with an exposure time of 90 s. The crystal was flash-cooled to 100 K in a stream of nitrogen gas using an Oxford Cryosystems Cryostream device, which allowed 116 data images to be collected from a single crystal with negligible radiation damage. Diffraction data for the RT−TNK-651 complex were collected from a single crystal and similarly flash-cooled to 100 K, on station BL19 at the ESRF, Grenoble, France, in October 1995 by the oscillation method using 1.5° oscillations. A total of 73 data frames, each with an exposure time of 90 s, were recorded using a 30 cm MAR Research imaging plate, programmed to collect in 18 cm mode, placed 230 mm from the crystal.

Auto indexing, spot measurement, and data reduction were performed with DENZO and SCALEPACK[58] (Table 1). The RT−MKC-442 data set was 95.6% complete for reflections with Bragg spacings from 30−2.55 Å. The RT−TNK-651 data set was 85.3% complete for reflections in the resolution range 20−2.55 Å. Both the RT−MKC-442 and RT−TNK-651 crystals were categorized as belonging to crystal form E,[47] having unit cell dimensions of a = 136.8 Å, b = 109.8 Å, c = 72.4 Å, and a = 137.3 Å, b = 110.2 Å, c = 72.1 Å, respectively.

Structure Determination and Refinement. Our model for the RT−nevirapine complex (refined against data to 2.2 Å)[22] (but excluding waters, the inhibitor and the RNaseH domain) was superposed, domain by domain, onto our unliganded RT model[47] which was solved in a crystal form similar to that of the RT−MKC-442 data. The RNaseH domain of the

unliganded RT was used unchanged (being better ordered than in the RT−nevirapine structure). This working model was refined against the RT−MKC-442 data: first treating the model as a single rigid body; then treating the p66 and p51 subunits as rigid groups (resolution range, 15−6 Å; *R* factor, 0.424 → 0.421); and finally using nine rigid groups corresponding to the individual domains (resolution range, 8−4 Å; *R* factor, 0.399 → 0.380). An $|F_{obs}| - |F_{calc}|$ difference map phased from this model clearly showed the MKC-442 bound in the NNI binding pocket and conformational changes to some residues. Positional refinement (resolution range, 10−2.55 Å; *R* factor, 0.418 → 0.320) and restrained individual atom *B* factor refinement (resolution range, 10−2.55 Å; *R* factor = 0.287) were followed by simulated annealing, positional, and *B* factor refinements (resolution range, 10−2.55 Å; *R* factor = 0.265). Further positional and *B* factor refinement with a bulk solvent correction gave an *R* factor of 0.246 for data from 25−2.55 Å resolution. All refinements were performed using X-PLOR.[59,60] Rounds of manual rebuilding, using FRODO[61] on an ESV workstation, alternated with simulated annealing refinement (with restrained individual temperature factor refinement and bulk solvent correction), resulted in the current model (see Table 1).

A well-refined intermediate model for the RT−MKC-442 complex (excluding water and inhibitor molecules) was used as an initial phasing model for the (nearly isomorphous) RT−TNK-651 data. The same rigid-body refinement protocols used for the RT−MKC-442 structure were employed to position the model in the cell (*R* factor = 0.342 for data in the range 10−2.55 Å). An $|F_{obs}| - |F_{calc}|$ difference map phased from this model showed the position of TNK-651 in the binding site and the movement of some protein residues. Positional refinement and restrained individual atom *B* factor refinement reduced the *R* factor to 0.290 (for data in the resolution range 10−2.55 Å). TNK-651 was incorporated into the model which was improved by rounds of simulated annealing and restrained individual atom *B* factor refinement (using a bulk solvent correction and data in the resolution range 20−2.55 Å) alternated with manual rebuilding using FRODO.[61] Water molecules were added to the model where electron density coincided with hydrogen bonding possibilities and a final round of positional and *B* factor refinement led to the current model (see Table 1).

The electron density maps are mostly well-defined, but a few short stretches of sequence appear to be disordered. For the MKC-442 complex model residues 540−560 from the p66 subunit and residues 1−5, 89−92, and 216−231 from the p51 subunit are omitted. For the TNK-651 model residues 544−560 from the p66 subunit and residues 1−5, 90−94, 212−231, and 433−440 from the p51 subunit are omitted. The coordinates for the RT−HEPT model have been deposited with the Protein Data Bank (1RTI). Coordinates for the RT−MKC-442 and RT−TNK-651 complexes have also been deposited and are scheduled for release 1 year from the date of publication.

Acknowledgment. We thank the staffs of the SRS, Daresbury Laboratory, U.K., and of the ESRF and EMBL outstation, Grenoble, France, for their help with data collection; Elspeth Garman for assistance in the development of cooling protocols; and Richard Bryan and Steven Lee for computing and photographic support. Part of this work has been supported by a British Council Collaborative Research Project (to H.T. and R.T.W.), and we are particularly indebted to Robin Sowden (Science Officer, Tokyo) for his interest and continuing support. The Oxford Centre for Molecular Sciences is supported by the BBSRC and MRC. E.Y.J. is supported by the Royal Society and D.I.S. by the MRC. The AIDS-directed program of the Medical Research Council has provided long-term funding for this project.

References

(1) Mitsuya, H.; Weinhold, K. J.; Furman, P. A.; St. Clair, M. H.; Nusinoff-Lehrman, S.; Gallo, R. C.; Bolognesi, D.; Barry, D. W.; Broder, S. 3′-Azido-3′-deoxythymidine (BW A509U): an antiviral agent that inhibits the infectivity and cytopathic effects of human T-lymphotrophic virus type III/lymphadenopathy-associated virus in vitro. *Proc. Natl. Acad. Sci. U.S.A.* **1985**, *82*, 7096−7100.

(2) Mitsuya, H.; Broder, S. Inhibition of in vitro infectivity and cytopathic effect of human T-lymphotrophic virus type III/lympadenopathy-associated virus (HTLV-III/LAV) by 2′,3′-dideoxynucleosides. *Proc. Natl. Acad. Sci. U.S.A.* **1986**, *83*, 1911−1915.

(3) Yarchoan, R.; Mitsuya, H.; Thomas, R. V.; Pluda, J. M.; Hartman, N. R.; Perno, C. F.; Marczyk, K. S.; Allain, J. P.; Johns, D. G.; Broder, S. In vivo activity against HIV and favorable toxicity profile of 2′,3′-dideoxyinosine. *Science* **1989**, *245*, 412−415.

(4) Coates, J. A. V.; Cammack, N.; Jenkinson, H. J.; Mutton, I. M.; Pearson, B. A.; Storer, R.; Cameron, J. M.; Penn, C. R. The separated enantiomers of 2′-deoxy-3′-thiacytidine (BCH-189) both inhibit human immunodeficiency virus replication in vitro. *Antimicrob. Agents Chemother.* **1992**, *36*, 202−205.

(5) St. Clair, M. H.; Richards, C. A.; Spector, T.; Weinhold, K. J.; Miller, W. H.; Langlois, A. J.; Furman, P. A. 3′-Azido-3′-deoxy thymidine triphosphate as an inhibitor and substrate of purified human immunodeficiency virus reverse transcriptase. *Antimicrob. Agents Chemother.* **1987**, *31*, 1972−1977.

(6) Fischl, M. A.; Richman, D. D.; Grieco, M. H.; Gottlieb, M. S.; Volberding, P. A.; Laskin, O. L.; Leedom, J. M.; Groopman, J. E.; Mildvan, D.; Schooley, R. T.; Jackson, G. G.; Durack, D. T.; King, D.; The AZT collaborative working group. The Efficacy of 3′-azido-3′-deoxythymidine (azidothymidine) in the treatment of patients with AIDS and AIDS-related complex. *N. Engl. J. Med.* **1987**, *317*, 185−191.

(7) Richman, D. D.; Fischl, M. A.; Grieco, M. H.; Gottleib, M. S.; Volberding, P. A.; Laskin, O. L.; Leedom, J. M.; Groopman, J. E.; Mildvan, D.; Hirsch, M. S.; Jackson, G. G.; Durack, D. T.; Nusinoff-Lehtman, S.; The AZT collaborative working group. The toxicity of azidothymidine (AZT) in treatment of patients with AIDS and AIDS-related complex. *N. Engl. J. Med.* **1987**, *317*, 192−197.

(8) Larder, B. A.; Kemp, S. D. Multiple mutations in HIV-1 reverse transcriptase confer high-level resistance to zidovudine (AZT). *Science* **1989**, *246*, 1155−1158.

(9) Larder, B. A.; Kemp, S. D.; Purifoy, D. J. M. Infectious potential of human immunodeficiency virus type 1 reverse transcriptase mutants with altered inhibitor sensitivity. *Proc. Natl. Acad. Sci. U.S.A.* **1989**, *86*, 4803−4807.

(10) Larder, B. A.; Darby, G.; Richman, D. D. HIV with reduced sensitivity to zidovudine (AZT) isolated during prolonged therapy. *Science* **1989**, *243*, 1731−1734.

(11) Baba, M.; Tanaka, H.; De Clercq, E.; Pauwels, R.; Balzarini, J.; Schols, D.; Nakashima, H.; Perno, C.-F.; Walker, R. T.; Miyasaka, T. Highly specific inhibition of human immunodeficiency virus type-1 by a novel 6-substituted acyclouridine derivative. *Biochem. Biophys. Res. Commun.* **1989**, *165*, 1375−1381.

(12) Merluzzi, V. J.; Hargrave, K. D.; Labadia, M.; Grozinger, K.; Skoog, M.; Wu, J. C.; Shih, C.-K.; Eckner, K.; Hattox, S.; Adams, J.; Rosenthal, A. S.; Faanes, R.; Eckner, R. J.; Koup, R. A.; Sullivan, J. L. Inhibition of HIV-1 replication by a nonnucleoside reverse transcriptase inhibitor. *Science* **1990**, *250*, 1411−1413.

(13) Goldman, M. E.; Nunberg, J. H.; O'Brien, J. A.; Quintero, J. C.; Schleif, W. A.; Freund, K. F.; Gaul, S. L.; Saari, W. S.; Wai, J. S.; Hoffman, J. M.; Anderson, P. S.; Hupe, D. J.; Emini, E. A.; Stern, A. M. Pyridinone derivatives: specific human immunodeficiency virus type 1 reverse transcriptase inhibitors with antiviral activity. *Proc. Natl. Acad. Sci. U.S.A.* **1991**, *88*, 6863−6867.

(14) Romero, D. L.; Busso, M.; Tan, C.-K.; Reusser, F.; Palmer, J. R.; Poppe, S. M.; Aristoff, P. A.; Downey, K. M.; So, A. G.; Resnick, L.; Tarpley, W. G. Nonnucleoside reverse transcriptase inhibitors that potently and specifically block human immunodeficiency virus type 1 replication. *Proc. Natl. Acad. Sci. U.S.A.* **1991**, *88*, 8806−8810.

(15) Pauwels, R.; Andries, K.; Desmyter, J.; Schols, D.; Kukla, M. J.; Breslin, H.J.; Raeymaeckers, A.; Gelder, J. V.; Woestenborghs, R.; Heykants, J.; Schellekens, K.; Janssen, M. A. C.; De Clercq, E.; Janssen, P. A. J. Potent and selective inhibition of HIV-1 replication in vitro by a novel series of TIBO derivatives. *Nature* **1990**, *343*, 470−474.

(16) Bader, J. P.; McMahon, J. B.; Schultz, R. J.; Narayanan, V. L.; Pierce, J. B.; Harrison, W. A.; Weislow, O. S.; Midelfort, C. F.; Stinson, S. F.; Boyd, M. R. Oxathiin carboxanilide, a potent inhibitor of human immunodeficiency virus replication. *Proc. Natl. Acad. Sci. U.S.A.* **1991**, *88*, 6740−6744.

(17) Frank, K. B.; Noll, G. J.; Connell, E. V.; Sim, I. S. Kinetic interaction of human immunodeficiency virus type 1 reverse transcriptase with the antiviral tetrahydroimidazo[4,5,1-jk]-[1,4]-benzodiazepine-2-(1H)-thioine compound R82150. *J. Biol. Chem.* **1991**, *266*, 14232−14236.

(18) Althaus, I. W.; Chou, J. J.; Gonzales, A. J.; Deibel, M. R.; Chou, K.-C.; Kezdy, F. J.; Romero, D. L.; Aristoff, P. A.; Tarpley, W. G.; Reusser, F. Steady-state kinetic studies with the non-nucleoside HIV-1 reverse transcriptase inhibitor U-87201E. *J. Biol. Chem.* **1993**, *268*, 6119−6124.

(19) Spence, R. A.; Kati, W. M.; Anderson, K. S.; Johnson, K. A. Mechanism of inhibition of HIV-1 reverse transcriptase by nonnucleoside inhibitors. *Science* **1995**, *267*, 988−993.

(20) Kohlstaedt, L. A.; Wang, J.; Friedman, J. M.; Rice, P. A.; Steitz, T. A. Crystal structure at 3.5 Å resolution of HIV-1 reverse transcriptase complexed with an inhibitor. *Science* **1992**, *256*, 1783−1790.

(21) Smerdon, S. J.; Jager, J.; Wang, J.; Kohlstaedt, L. A.; Chirino, A. J.; Friedman, J. M.; Rice, P. A.; Steitz, T. A. Structure of the binding site for nonnucleoside inhibitors of the reverse transcriptase of human immunodeficency virus type 1. *Proc. Natl. Acad. Sci. U.S.A.* **1994**, *91*, 3911−3915.

(22) Ren, J. S.; Esnouf, R.; Garman, E.; Jones, Y.; Somers, D.; Ross, C.; Kirby, I.; Keeling, J.; Darby, G.; Stuart, D.; Stammers, D. High resolution structure of HIV-1 RT: insights from four RT-inhibitor complexes. *Nature Struct. Biol.* **1995**, *2*, 293−302.

(23) Ding, J.; Das, K.; Tantillo, C.; Zhang, W.; Clark, A. D. J.; Jessen, S.; Lu, X.; Hsiou, Y.; Jacobo-Molina, A.; Andries, K.; Pauwels, R.; Moereels, H.; Koymans, L.; Janssen, P. A. J.; Smith, R. H. J.; Kroeger Koepke, R.; Michejda, C. J.; Hughes, S. H.; Arnold, E. Structure of HIV-1 reverse transcriptase in a complex with the non-nucleoside inhibitor α-APA R 95845 at 2.8 Å resolution. *Structure* **1995**, *3*, 365−379.

(24) Ding, J.; Das, K.; Moereels, H.; Koymans, L.; Andries, K.; Janssen, P. A. J.; Hughes, S. H.; Arnold, E. Structure of HIV-1 RT/TIBO R 86183 complex reveals similarity in the binding of diverse nonnucleoside inhibitors. *Nature Struct. Biol.* **1995**, *2*, 407−415.

(25) Ren, J. S.; Esnouf, R.; Hopkins, A.; Ross, C.; Jones, Y.; Stammers, D.; Stuart, D. The structure of HIV-1 reverse transcriptase complexed with 9-chloro-TIBO: lessons for inhibitor design. *Structure* **1995**, *3*, 915−926.

(26) Yuasa, S.; Sadakata, Y.; Takashima, H.; Sekiya, K.; Inouye, N.; Ubasawa, M.; Baba, M. Selective and synergistic inhibition of human immunodeficiency virus type 1 reverse transcriptase by a non-nucleoside inhibitor, MKC-442. *Mol. Pharmacol.* **1993**, *44*, 895−900.

(27) Richman, D.; Shih, C.-K.; Lowy, I.; Rose, J.; Prodanovich, P.; Goff, S.; Griffin, J. Human immunodeficiency virus type 1 mutants resistant to non-nucleoside inhibitors of reverse transcriptase arise in tissue culture. *Proc. Natl. Acad. Sci. U.S.A.* **1991**, *88*, 11241−11245.

(28) Richman, D. D.; Havlir, D.; Corbeil, J.; Looney, D.; Ignacio, C.; Spector, S.A.; Sullivan, J.; Cheeseman, S.; Barringer, K.; Pauletti, D.; Shih, C.-K.; Myers, M.; Griffin, J. Nevirapine resistance mutations of human immunodeficiency virus type 1 selected during therapy. *J. Virol.* **1994**, *68*, 1660−1666.

(29) Schinazi, R.; Larder, B.; Mellors, J. Mutations in HIV-1 reverse transcriptase and protease associated with drug resistance. *Int. Antiviral News* **1994**, *2*, 72−75.

(30) Bebenek, K.; Kunkel, T. A. The fidelity of retrovial reverse transcriptase. In *Reverse Transcriptase*; Skalka, A. M., Goff, S. P., Eds.; Cold Spring Harbor Press: New York, **1993**; pp 85−102.

(31) Wei, X.; Ghosh, S. K.; Taylor, M. E.; Johnson, V. A.; Emini, E. A.; Deutsch, P.; Lifson, J. D.; Bonhoeffer, S.; Nowak, M. A.; Hahn, B. H.; Saag, M. S.; Shaw, G. M. Viral dynamics in human immunodeficiency virus type 1 infection. *Nature* **1995**, *373*, 117−122.

(32) Coffin, J. HIV population dynamics in vivo: implications for genetic variation, pathogenesis, and therapy. *Science* **1995**, *267*, 483−489.

(33) Larder, B. A. 3′-Azido-3′-deoxythymidine resistance suppressed by a mutation conferring human immunodeficiency virus type 1 resistance to nonnucleoside reverse transcriptase inhibitors. *Antimicrob. Agents Chemother.* **1992**, *36*, 2664−2669.

(34) Larder, B. A. Interactions between drug resistance mutations in human immunodeficiency virus type 1 reverse transcriptase. *J. Gen. Virol.* **1994**, *75*, 951−957.

(35) Pauwels, R.; Andries, K.; Debyser, Z.; Van Daele, P.; Schols, D.; Stoffels, P.; De Vreese, K.; Woestenborghs, R.; Vandamme, A.-M.; Janssen, C. G. M.; Anne, J.; Cauwenbergh, G.; Desmyter, J.; Heykants, J.; Janssen, M. A. C.; De Clercq, E.; Janssen, P. A. J. Potent and highly selective HIV-1 inhibition by a new series of α-anilinophenylacetamide α-APA derivatives targeted at HIV-1 reverse transcriptase. *Proc. Natl. Acad. Sci. U.S.A.* **1993**, *90*, 1711−1715.

(36) Hargrave, K. D.; Proudfoot, J. R.; Grozinger, K. G.; Cullen, E.; Kapadia, S. R.; Patel, U. R.; Fuchs, V. U.; Mauldin, S. C.; Vitous, J.; Behnke, M. L.; Klunder, J.M.; Pal, K.; Skiles, J. W.; McNeil, D. W.; Rose, J. M.; Chow, G. C.; Skoog, M. T.; Wu, J. C.; Schmidt, G.; Engel, W. W.; Eberlein, W. G.; Saboe, T. D.; Campbell, S. J.; Rosenthal, A. S.; Adams, J. Novel non-nucleoside inhibitors of HIV-1 reverse transcriptase. 1. Tricyclic pyridobenzo- and dipyridodiaze-pinones. *J. Med. Chem.* **1991**, *34*, 2231−2241.

(37) Baba, M.; De Clercq, E.; Tanaka, H.; Ubasawa, M.; Takashima, H.; Sekiya, K.; Nitta, I.; Umezu, K.; Nakashima, H.; Mori, S.; Shigeta, S.; Walker, R. T.; Miyasaka, T. Potent and selective inhibition of human immunodeficiency virus type 1 (HIV-1) by 5-ethyl-6-phenylthiouracil derivatives through their interaction with HIV-1 reverse trancriptase. *Proc. Natl. Acad. Sci. U.S.A.* **1991**, *88*, 2356−2360.

(38) Baba, M.; De Clercq, E.; Tanaka, H.; Ubasawa, M.; Takashima, H.; Sekiya, K.; Nitta, I.; Umezu, K.; Walker, R. T.; Mori, S.; Ito, M.; Shigeta, S.; Miyasaka, T. Highly potent and selective inhibition of human immunodeficiency virus type 1 (HIV-1) by a novel series of 6-substituted acyclouridine derivatives. *Mol. Pharmacol.* **1991**, *39*, 805−810.

(39) Tanaka, H.; Baba, M.; Hayakawa, H.; Sakamaki, T.; Miyasaka, T.; Ubasawa, M.; Takashima, H.; Sekiya, K.; Nitta, I.; Shigeta, S.; Walker, R. T.; Balzarini, J.; De Clercq, E. A new class of HIV-1-specific 6-substituted acyclouridine derivatives: synthesis and anti-HIV-1 activity of 5- or 6-substituted analogues of 1-[(2-hydroxyethoxy)methyl]-6-(phenylthio)thymine (HEPT). *J. Med. Chem.* **1991**, *34*, 349−357.

(40) Baba, M.; Shigeta, S.; Tanaka, H.; Miyasaka, T.; Ubasawa, M.; Umezu, K.; Walker, R. T.; Pauwels, R.; De Clercq, E. Highly potent and selective inhibition of HIV-1 replication by 6-phenylthiouracil derivatives. *Antiviral Res.* **1992**, *17*, 245−264.

(41) Miyasaka, T.; Tanaka, H.; Baba, M.; Hayakawa, H.; Walker, R. T.; Balzarini, J.; De Clercq, E. A novel lead for specific anti-HIV-1 agents: 1-[(2-hydroxyethoxy)methyl]-6-(phenylthio)thymine. *J. Med. Chem.* **1989**, *32*, 2507−2509.

(42) Baba, M.; Shigeta, S.; Yuasa, S.; Takashima, H.; Sehiya, K.; Ubasawa, M.; Tanaka, H.; Miyasaka, T.; Walker, R. T.; De Clercq, E. Preclinical evaluation of MKC-442, a highly potent and specific inhibitor of human immunodeficiency virus type 1 in vitro. *Antimicrob. Agents Chemother.* **1994**, *38*, 688−692.

(43) Balzarini, J.; Karlsson, A.; De Clercq, E. Human immunodeficiency virus type 1 drug-resistance patterns with different 1-[(2-hydroxyethoxy)methyl]-6-(phenylthio)thymine derivatives. *Mol. Pharmacol.* **1993**, *44*, 694−701.

(44) Seki, M.; Sadakata, Y.; Yuasa, S.; Baba, M. Isolation and characterisation of human immunodeficiency virus type-1 mutants resistant to the non-nucleoside reverse transcriptase inhibitor MKC-442. *Antiviral Chem. Chemother.* **1995**, *6*, 73−79.

(45) Nicholls, A.; Sharp, K.; Honig, B. Protein folding and association: insights from the interfacial and thermodynamic properties of hydrocarbons. *Proteins* **1991**, *11*, 281−296.

(46) Rodgers, D. W.; Gamblin, S. J.; Harris, B. A.; Ray, S.; Culp, J. S.; Hellmig, B.; Woolf, D. J.; Debouck, C.; Harrison, S. C. The structure of unliganded reverse transcriptase from the human immunodeficiency virus type 1. *Proc. Natl. Acad. Sci. U.S.A.* **1995**, *92*, 1222−1226.

(47) Esnouf, R.; Ren, J. S.; Ross, C.; Jones, Y.; Stammers, D.; Stuart, D. Mechanism of inhibition of HIV-1 reverse transcriptase by non-nucleoside Inhibitors. *Nature Struct. Biol.* **1995**, *2*, 303−308.

(48) Tanaka, H.; Baba, M.; Ubasawa, M.; Takashima, H.; Sekiya, K.; Nitta, I.; Shigeta, S.; Walker, R. T.; De Clercq, E.; Miyasaka, T. Synthesis and anti-HIV-1 activity of 2-, 3-, and 4-substituted analogues of 1-[(2-hydroxyethoxy)methyl]-6-(phenylthio)thymine (HEPT). *J. Med. Chem.* **1991**, *34*, 1394−1399.

(49) Tanaka, H.; Baba, M.; Saito, S.; Miyasaka, T.; Takashima, H.; Sekiya, K.; Ubasawa, M.; Nitta, I.; Walker, R. T.; Nakashima, H.; De Clercq, E. Specific anti-HIV-1 "acyclonucleosides" which cannot be phosphorylated: synthesis of some deoxy analogues of 1-[(2-hydroxyethoxy)methyl]-6-(phenylthio)thymine. *J. Med. Chem.* **1991**, *34*, 1508−1511.

(50) Tanaka, H.; Takashima, H.; Ubasawa, M.; Sekiya, K.; Nitta, I.; Baba, M.; Shigeta, S.; Walker, R. T.; De Clercq, E.; Miyasaka, T. Structure-activity relationships of 1-[(2-hydroxyethoxy)-methyl]-6-(phenylthio)thymine analogues: effects of substituents at the C-6 phenyl ring and at the C-5 position on anti-HIV-1 activity. *J. Med. Chem.* **1992**, *35*, 337−345.

(51) Tanaka, H.; Takashima, H.; Ubasawa, H.; Sekiya, K.; Nitta, I.; Baba, M.; Shigeta, S.; Walker, R. T.; De Clercq, E.; Miyasaka, T. Synthesis and antiviral activity of deoxy analogues of 1-[(2-hydroxyethoxy)methyl]-6-(phenylthio)-thymine (HEPT) as potent and selective anti-HIV-1 agents. *J. Med. Chem.* **1992**, *35*, 4713−4719.

(52) Boyer, P. L.; Currens, M. J.; McMahon, J. B.; Boyd, M. R.; Hughes, S. H. Analysis of nonnucleoside drug-resistant variants of human immunodeficiency virus type 1 reverse transcriptase. *J. Virol.* **1993**, *67*, 2412−2420.

(53) Dueweke, T. J.; Pushkarskaya, T.; Poppe, S. M.; Swaney, S. M.; Zhao, J. Q.; Chen, I. S. Y.; Stevenson, M.; Tarpley, W. G. A mutation in reverse transcriptase of bis(heteroaryl)piperazine-resistant human immunodeficiency virus type 1 that confers increased sensitivity to other nonnucleoside inhibitors. *Proc. Natl. Acad. Sci. U.S.A.* **1993**, *90*, 4713−4717.

(54) Baba, M.; De Clercq, E.; Iida, S.; Tanaka, H.; Nitta, I.; Ubasawa, M.; Takashima, H.; Sekiya, K.; Umezu, K.; Nakashima, H.; Shigeta, S.; Walker, R. T.; Miyasaka, T. Anti-HIV-1 activities and pharmacokinetics of novel 6-substituted acyclouridine derivatives. *Antimicrob. Agents Chemother.* **1990**, *34*, 2358−2363.
(55) Kleim, J.-P.; Bender, R.; Kirsch, R.; Meichsner, C.; Paessens, A.; Riess, A.G. Mutational analysis of residue 190 of human immunodeficiency virus reverse transcriptase. *Virology* **1994**, *200*, 696−701.
(56) Tanaka, H.; Takashima, H.; Ubasawa, M.; Sekiya, K.; Inouye, N.; Baba, M.; Shigeta, S.; Walker, R. T.; De Clercq, E.; Miyasaka, T. Synthesis and antiviral activity of 6-benzyl analogs of 1-[(2-hydroxyethoxy)methyl]-6-(phenylthio)thymine (HEPT) as potent and selective anti-HIV-1 agents. *J. Med. Chem.* **1995**, *38*, 2860−2865.
(57) Stammers, D. K.; Somers, D. O'N.; Ross, C. K.; Kirby, I.; Ray, P. H.; Wilson, J. E.; Norman, M.; Ren, J. S.; Esnouf, R. M.; Garman, E. F.; Jones, E. Y.; Stuart, D. I. Crystals of HIV-1 reverse transcriptase diffracting to 2.2 Å resolution. *J. Mol. Biol.* **1994**, *242*, 586−588.
(58) Otwinowski, Z. Oscillation data reduction program. In *Data collection and Processing*; Sawyer, L., Isaacs, N., Bailey, S., Eds.; SERC Daresbury Laboratory: Warrington, England, 1993; pp 56−62.
(59) Brünger, A. T.; Krukowski, A.; Erickson, J. Slow-cooling protocols for crystallographic refinement by simulated annealing. *Acta Crystallogr.* **1990**, *A46*, 585−593.
(60) Brünger, A. T. *X-PLOR Manual*, Version 3.1; Yale University: New Haven, CT, 1992.
(61) Jones, T. A. Interactive computer graphics: FRODO. *Meth. Enzymol.* **1985**, *115*, 157−171.
(62) Laskowski, R. A.; MacArthur, M. W.; Moss, D. S.; Thornton, J. M. PROCHECK: a program to check the stereochemical quality of protein structures. *J. Appl. Crystallogr.* **1993**, *26*, 283−291.
(63) Kraulis, P. J. MOLSCRIPT: a program to produce both detailed and schematic plots of protein structures. *J. Appl. Crystallogr.* **1991**, *24*, 946−950.
(64) Merritt, E. A.; Murphy, M. E. P. Raster3D version 2.0. A program for photorealistic molecular graphics. *Acta Crystallogr.* **1994**, *D50*, 869−873.
(65) Stuart, D. I.; Levine, M.; Muirhead, H.; Stammers, D. K. The crystal structure of cat pyruvate kinase at a resolution of 2.6 Å. *J. Mol. Biol.* **1979**, *134*, 109−142.

JM960056X